

## **Lower ionosphere influenced by high-class Solar flare events as observed through VLF measurements**

**Aleksandra Kolarski**

*Institute of Physics Belgrade, University of Belgrade, Pregrevica 118, 11000  
Belgrade, Serbia*

*E-mail: aleksandra.kolarski@ipb.ac.rs*

### **Abstract**

Solar flare events, the powerful explosions on Sun, are one of the most significant drivers of the lower ionospheric behavior related to solar activity. During occurrence of solar flare events, emanated electromagnetic energy within X-ray radiation of soft range (0.1-0.8 nm) impacts Earth within only several minutes, passing through the Earth's atmosphere and reaching D-region altitudes (50-90 km), causing ionization of its constituents on the sunlit side of the Earth. Additional ionization ultimately leads to perturbations of the Very Low Frequency (VLF) radio signals (3-30 kHz) propagating within Earth-ionosphere waveguide, forcing them to divert from their regular propagation patterns, making the remote sensing of the lower Ionosphere using the ground-based network of stations as a research method of choice for exploration of this region. High-class solar flare events during the last two solar cycles (SCs) and their impacts on the lower ionosphere based on VLF technology were subject of this research. Particular focus was on the strongest among these events, including the September 2017 events, as recorded by VLF station in Belgrade (44.85N, 20.38W), Serbia. For modeling purposes the Long Wave Propagation Capability (LWPC) software was used. Some of the most relevant parameters related to numerical simulations of VLF propagation characteristics under the high-class Solar flare events are given.

### **Introduction**

Ionized constituents within Earth's atmosphere are grouped within several ionospheric layers, with the D-region reaching the altitudes from 50 to 90 km as the lowest one. Properties of ionospheric plasma constituents within these layers are significantly different both in their characteristics, as well as in variation features, ionization processes, spatial and temporal distribution of the concentrations etc. (e.g. Bilitza et al. 2017, Wait and Spies 1964). During perturbed solar conditions related to flare activity, portion of X-ray radiation from released Sun's energy of electromagnetic spectrum causes additional ionization of neutral

constituents within the altitude range corresponding to D-region and significantly alters ionization rates compared to these of lower ionospheric ionizing agents during the regular conditions, such as Lyman-  $\alpha$  spectral line and cosmic rays (e.g. Whitten and Poppoff 1965, Hargreaves 1992, Thomson et al. 2021). As a consequence of such increased additional ionization, electron densities within this region are increased as well (Mitra et al. 1974), directly affecting subionospheric Very Low Frequency (VLF) signal transmission that is otherwise stable under the regular ionospheric conditions (e.g. Budden 1988, Thomson 1993, McRae and Thomson 2000). However, it is important to note that D-region, as the closest one to the Earth's surface, in addition to extraterrestrial influences, is also directly affected by different terrestrial processes as well (review of some of the major drivers and also regarding the possibilities of VLF methodology application for such purposes can be found in e.g. Silber and Price 2017).

Since released from U. S. military into the public sector in the late 90s, Long Wave Propagation Capability (LWPC) software (Ferguson et al. 1998), has a long history of successful applications for numerous and diverse purposes related to lower ionospheric explorations. Employing real measurements originating from VLF technology, as a remote sensing technique on one hand, and relaying on Wait's theory (Wait and Spies 1964, Wait 1970) on the other, this numerical method has been widely utilized and is proven as a reliable method for indirect obtaining of lower ionospheric parameters (e.g. Thomson et al. 2005, McRae and Thomson 2004, Žigman et al. 2023, Grubor et al. 2008, Nina et al. 2018, Kolarski et al. 2022, 2023, Kumar and Kumar 2018, Šulić and Srećković 2014, Srećković et al. 2021, Chowdhury et al. 2021, Bekker et al. 2021 etc.).

High-class solar flares (SFs) of X-class, from period covering 23<sup>rd</sup> – 25<sup>th</sup> solar cycle (SC) were examined, in terms of their influence on the lower ionosphere electron density changes, indirectly through retrieving of VLF parameters of subionospherically propagating radio signals, as recorded by different ground-based stations globally positioned and as observed on VLF signals with different Great Circle Paths (GCPs). Focus was placed on the strongest events, among which these from September 2017, as recorded by Belgrade VLF station (44.85N, 20.38W) in Serbia, are given in more detail. For simulation of both unperturbed and perturbed lower ionospheric conditions due to X-class SFs, LWPC numerical modeling procedure was applied.

## Analysis and results

X-class SFs are events with X-ray irradiance greater than  $10^{-4} \text{ Wm}^{-2}$  and are the most powerful SF events within current classification (that groups all events from A- being the smallest to X- being the largest class). In general, X-class SFs are more common in appearance around periods of solar maximum or ascending and/or descend intervals near maximum of SC, compared to other periods as these related to minimum of solar activity.

However, one of the examples that powerful SF events can occur regardless the stage within the cycle of solar activity are exactly the examples of SFs from September 2017 (Figure 1), when within just a few days several intense SFs ranging from M5.5 to X9.3 occurred inspire the fact that SC progression was in descending stage getting close to the minimum of solar activity (which took place in December 2019) between 24<sup>th</sup> and 25<sup>th</sup> - i.e the current SC. During September 2017, 4 X-class SFs in range X1.3 – X9.3 occurred on 6<sup>th</sup>, 7<sup>th</sup> and 10<sup>th</sup>, while 2 high M-class events of M7.3 and M8.1 occurred on 7<sup>th</sup> and 8<sup>th</sup> September 2017. It is of significance to point out that X9.3 event from 6<sup>th</sup> September 2017 was the strongest SF within 24<sup>th</sup> SC. An overview of high X-class ( $\geq X5.0$ ) SF events in period of last two SCs are given in Table 1, as for the sake of visibility are listed by the year of their occurrence rather than their intensity, which is indicated in separate columns on the left. During current SC, there were no high X-class SF events reported as per 15<sup>th</sup> August 2023. Lower to moderate X-class (X1-X4.9) SF events from 23<sup>rd</sup> to 25<sup>th</sup> SC are given in Table 2, including data ending with 15<sup>th</sup> August 2023, as well. September 2017 events are emphasized in bold font. According to National Oceanic and Atmospheric Administration (NOAA), solar X-ray xflux data were obtained from the Geostationary Operational Environmental Satellite (GOES) Network database.

Response of the lower ionosphere to influence of intense SF events of X-class is modeled based on propagation parameters of VLF radio signals, known as Wait's parameters: effective reflection height  $H'$  (km) and reflection height sharpness  $\beta$  (km<sup>-1</sup>), used for calculation of corresponding electron densities  $N_e$  (m<sup>-3</sup>) within D-region altitude range, using equation obtained based on Wait's theory which applies for daytime ionospheric conditions:

$$N_e(z, H', \beta) = 1.43 \cdot 10^{13} \cdot e^{-0.15H'} \cdot e^{(\beta-0.15)(z-H')} \quad (1)$$

Wait's parameters  $H'$  (km) and  $\beta$  (km<sup>-1</sup>) in function of X-ray flux soft component, as measured by GOES satellite probes, for different cases of high-class SFs, with X-class region marked by shaded gray area, are given in Figures 2 and 3. Estimated corresponding electron densities  $N_e$  (m<sup>-3</sup>) in function of X-ray flux soft component, indirectly obtained by the use of numerical modeling procedure employing LWPC software by modeling of propagation parameters of VLF signals, are given in Figure 4 (X-class region is also marked by shaded gray area. Results corresponding to output from numerical modeling conducted in this research and related to events from 6<sup>th</sup> September 2017, are presented by black stars. Wait's parameters  $\beta$  (km<sup>-1</sup>) and  $H'$  (km), obtained through numerical modeling procedure, that correspond to peaks of X-ray fluxes of analyzed SFs changed as follows: for X2.2 SF  $\uparrow \Delta\beta = 0.13 \text{ km}^{-1}$  and  $\downarrow \Delta H' = 14 \text{ km}$  and for X9.3 SF  $\uparrow \Delta\beta = 0.25 \text{ km}^{-1}$  and  $\downarrow \Delta H' = 15.6 \text{ km}$ , compared to pair of predefined unperturbed values of  $(\beta; H') = (0.3; 74)$  characteristic for daytime ionospheric

regular conditions. Based upon conducted calculations for entire altitude range of D-region,  $Ne$  for analyzed SFs differs within one order of magnitude throughout the entire D-region. At reference height of 74 km, compared to regular ionospheric conditions, in case of X2.2 SF  $Ne$  showed increase by almost 3 and in case of X9.3 SF about 3.5 orders of magnitude.

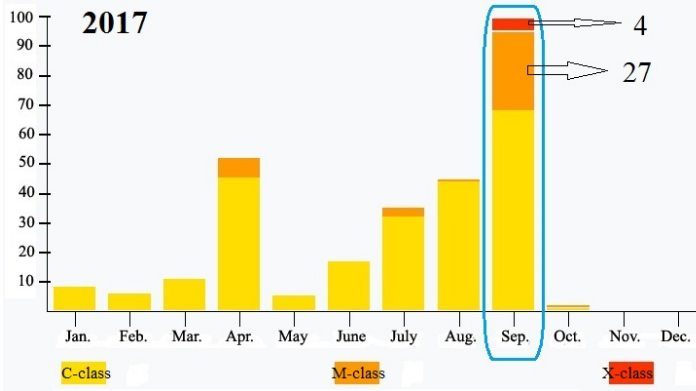


Fig. 1. SFs occurred during 2017, with September events highlighted by blue oval: 4 X- and 27 M-class SFs were reported according to NOAA.

Table 1. SFs of higher X-class ( $\geq X5.0$ ) from 23<sup>rd</sup> to 25<sup>th</sup>\* SC.

X-class SFs	SC 23: Aug. 1996 – Dec. 2008 (left: strength in SC, right: SF)		SC 24: Dec. 2008 – Dec. 2019 (left: strength in SC, right: SF)	
$\geq X5.0$	7	X9.4; 1997-11-06; 11:55UT		
	14	X5.7; 2000-07-14; 10:24UT		
	2	X20+; 2001-04-02; 21:51UT		
	5	X14.4; 2001-04-15; 13:50UT		
	13	X6.2; 2001-12-13; 14:30UT		
	15	X5.6; 2001-04-06; 19:21UT	3	X6.9; 2011-08-09; 08:05UT
	18	X5.3; 2001-08-25; 16:45UT	4	X5.4; 2012-03-07; 00:24UT
	1	X28+; 2003-11-04; 19:53UT	1	<b>X9.3; 2017-09-06; 12:02UT</b>
	3	X17.2+; 2003-10-28; 11:10UT	2	<b>X8.2; 2017-09-10; 16:06UT</b>
	6	X10; 2003-10-29; 20:49UT		
	9	X8.3; 2003-11-02; 17:25UT		
	17	X5.4; 2003-10-3; 08:35UT		
	4	X17+; 2005-09-07; 17:40UT		
10		X7.1; 2005-01-20; 07:01UT		

	12	X6.2; 2005-09-09; 20:04UT		
	16	X5.4; 2005-09-08; 21:06UT		
	8	X9; 2006-12-05; 10:35UT		
	11	X6.5; 2006-12-06; 18:47UT		

\* Including data ending with 2023-08-15: no  $\geq$ X5 class SFs in SC 25

Table 2. SFs of lower to moderate X-class (X1-X4.9) from 23<sup>rd</sup> to 25<sup>th</sup>\* SC.

1997: 2 SFs in range X2.1-X2.6 1998: 14 SFs in range X1-X4.9 1999: 4 SFs in range X1.1-X1.8 2000: 16 SFs in range X1-X4 2001: 16 SFs in range X1-X3.4 2002: 11 SFs in range X1-X4.8 2003: 15 SFs in range X1-X3.9 2004: 12 SFs in range X1-X3.6 2005: 14 SFs in range X1.1-X3.8 2006: 2 SFs in range X1.5-X3.4	SC 23: Aug. 1996 – Dec. 2008
2011: 7 SFs in range X1.4-X2.2 2012: 6 SFs in range X1.1-X1.8 2013: 12 SFs in range X1-X3.3 2014: 16 SFs in range X1-X4.9 2015: 2 SFs in range X2.2-X2.7 <b>2017: 2 SFs in range X1.3-X2.2</b>	SC 24: Dec. 2008 – Dec. 2019
2021: 2 SFs in range X1-X1.59 2022: 7 SFs in range X1-X2.2 2023: 11 SFs in range X1-X2.28	SC 25: Dec. 2019 – first half 2034 (pred.)

\* Including data ending with 2023-08-15

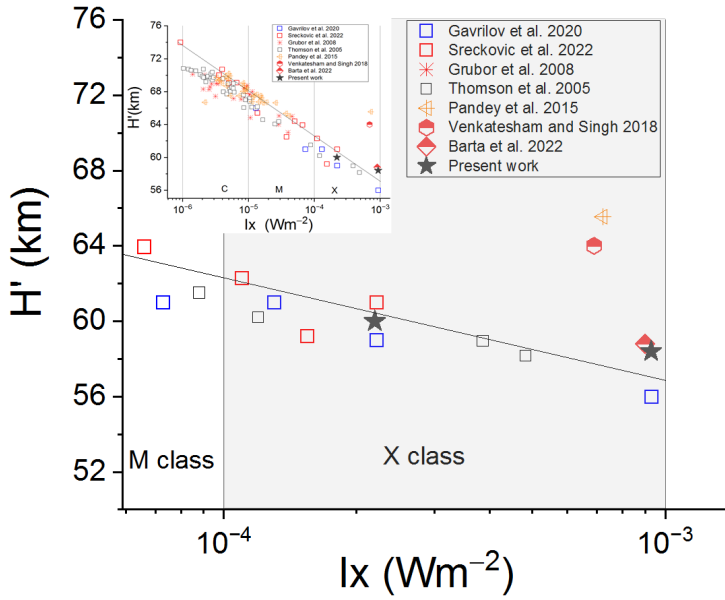


Fig. 2. Parameter  $H'$  (km) in function of X-ray flux soft component.

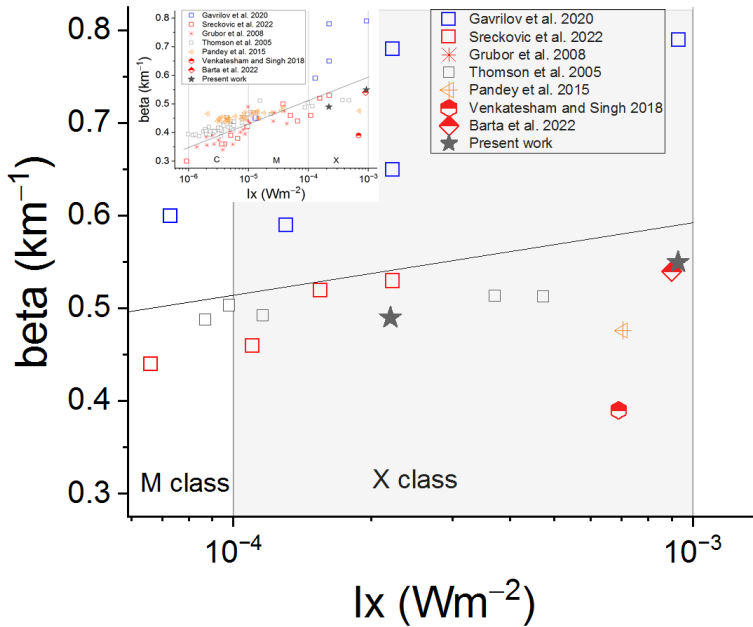


Fig. 3. Parameter  $\beta$  (km<sup>-1</sup>) in function of X-ray flux soft component.

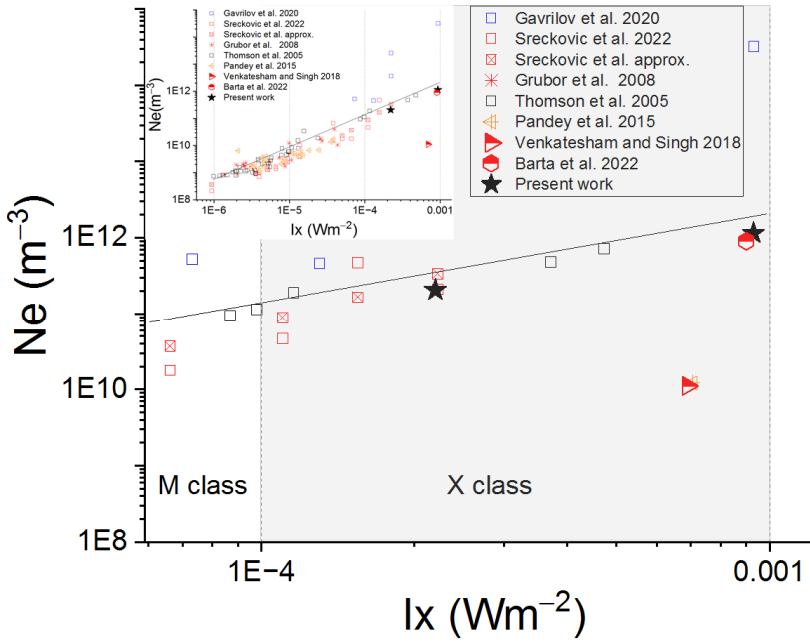


Fig. 4. Estimated electron densities  $Ne \text{ (m}^{-3}\text{)}$ , obtained based on conducted numerical modeling procedure, in function of X-ray flux soft component.

## Discussion and conclusions

Modeling of high-class SF events is a challenging task, due to their high strength that usually mirrors itself onto lower ionospheric response through a large scale VLF signal perturbations, which are not easily modeled using numerical procedure employing LWPC software package, especially taking into consideration LWPC software limitations related to waveguide border boundaries. Results from this research regarding Wait's parameters and estimated electron densities related to one weak X2.2 and other strong X9.3 X-class SF occurred on 6<sup>th</sup> September 2017 were compared with results available from other studies dealing with major cases of strong SFs across three past SCs. Comparison is done for period 2003-2011 including SF cases of class X28+ – X6.9 (1-4) and with some other cases from period 2006-2017 covering range X1 – X9.3 (5-9) and from period 1994-1998 in range X1 – X5 (10), recorded by equipment located in different latitudinal sectors:

- 1) X6.9 of 09-08-2011 at 08:05UT – strongest SF of 24<sup>th</sup> SC, associated with CME and SPE events; at low-latitude site in India: values of obtained Wait's parameters  $H' \sim 64.0 \text{ km}$  and  $\beta \sim 0.39 \text{ km}^{-1}$ , which decreases  $H'$  by 10 km, and increases  $\beta$  by  $0.09 \text{ km}^{-1}$ , compared to unperturbed conditions (Venkatesham

- and Singh 2018) and  $H'=65.7$  km and  $\beta=0.48$  km<sup>-1</sup>, compared unperturbed values of  $H'=71.0$  km and  $\beta=0.43$  km<sup>-1</sup> (Pandey et al. 2015).
- 2) X9 of 05-12-2006 at 10:35UT – strongest SF in 2006 and eighth of 23<sup>rd</sup> SC; at mid-latitude site - Belgrade VLF database: values of obtained Wait's parameters related to X9 are  $H'=58.8$  km and  $\beta=0.54$  km<sup>-1</sup>, electron density changes reach even 3 orders of magnitude at height of 70 km. (Barta et al. 2022).
  - 3) X28+ of 04-11-2003 at 19:53UT – one of strongest solar flares ever recorded and strongest of 23<sup>rd</sup> SC associated with CME and SPE events, from very active period October 20<sup>th</sup> - November 5<sup>th</sup>, 2003 including X10.1 of October 29<sup>th</sup>, 2003 at 20:49UT and X8.3 of November 2<sup>nd</sup>, 2003 at 17:25UT third and fourth in 2003 and sixth and ninth of 23<sup>rd</sup> SC, both associated with CME; at mid-latitude site at Dunedin, New Zealand: values of obtained Wait's parameters related to X28+ are  $H'$  had lowered to a height of about 53 km, or about 17 km below value of  $H'=71$  km typical for unperturbed conditions and  $\beta$  increased up to about 0.57 compared to unperturbed value of  $\beta=0.39$  km<sup>-1</sup>. These results were obtained through analysis of a series of SFs from the same very active solar period from 20-10-2003 to 05-11-2003, that included X28+ of 04-11-2003 at 19:53UT, X17.2 of 28-10-2003 at 11:00UT and X10 of 29-10-2003 at 20:49UT and also X8.3 on 02-11-2003 at 17:25UT, and X5.4 on 23-10-2003 at 08:35UT, and X3.9 on 03-11-2003 at 09:55UT. Also were included SF events X20+ of 02-04-2001 at 21:51UT, X9.4 of 06-11-1997 at 11:55UT and X1.3 on 27-05-2003 at 23:07UT, 06-11-1997 (X9), 18-08-1998 (X5), 14-07-2000 (X6), 2-, 6- and 15-04-2001 (X20, X5.6, X14), 28-08-2001, 13-12-2001 (X5, X6) and 23-07-2002 (X5). Events X17.2+ of 28-10-2003 at 11:10UT and X14.4 of 15-04-2001 at 13:50UT were excluded due to receiver location (Thomson et al. 2005).
  - 4) X7.1 of 20-01-2005 at 07:01UT – second strongest SF in 2005 and tenth of 23<sup>rd</sup> SC associated with CME and SPE events, from active period January 15<sup>th</sup>–22<sup>nd</sup>, 2005; at mid-latitude site - Belgrade VLF database: obtained Wait's parameters related to X7.1 depend on signal GCP,  $H'$  descended for 7 km and  $Ne$  increased for 2 orders of magnitude compared to regular conditions (unperturbed values of 74 km and  $2.16 \cdot 10^8$  m<sup>-3</sup>) (Grubor et al. 2007),  $\beta=0.6$  km<sup>-1</sup> and  $H'=70$  km corresponding to  $Ne$  increase of about 1.5 orders of magnitude compared to unperturbed midday conditions (Kolarski and Grubor 2021) and  $\beta=0.38$  km<sup>-1</sup> and  $H'=61$  km with  $Ne(74) \sim 2 \cdot 10^{10}$  m<sup>-3</sup> (Žigman et al. 2023).
  - 5) X1.1-X2.2 of 10- and 11-06-2014 (CME?) & X17.2 of October 28<sup>th</sup>, 2003 (associated with CME and SPE events); at mid-latitude site - Belgrade VLF database: values of obtained Wait's parameters related to X2.2 of 2014-06-10 at 11:42UT are  $\beta=0.52$  km<sup>-1</sup> and  $H'=59.2$  km with  $Ne=4.75 \cdot 10^{11}$  m<sup>-3</sup>, for X1.5 of 2014-06-10 at 12:52UT are  $\beta=0.53$  km<sup>-1</sup>,  $H'=61.0$  km with  $Ne=2.12 \cdot 10^{11}$  m<sup>-3</sup>, for X1.1 of 2014-06-11 at 09:06UT are  $\beta=0.46$  km<sup>-1</sup>,  $H'=62.3$  km and  $Ne=4.70 \cdot 10^{10}$  m<sup>-3</sup> and for X17.2 of 2003-10-28 at 11:10UT  $Ne$  was estimated as reaching value of about  $0.7 \cdot 10^{13}$  m<sup>-3</sup> (Srećković et al. 2021).



- 6) X1.3 of 07-09-2017; at mid-latitude site - Belgrade VLF database: values of obtained Wait's parameters related to X1.3 are  $\beta=0.42 \text{ km}^{-1}$ ,  $H'=63 \text{ km}$  and  $N_e$  increased almost two orders of magnitude compared to the regular value at altitude 74 km (Kolarski et al. 2022).
- 7) X1.3-X9.3 of 10-06-2014 and 6- to 10-09-2017, with strongest two of them (both above X5) associated with CME; at mid-latitude site at Mikhnevo in Russia, a bit northward from Belgrade and for hard component of X-ray flux: values of obtained Wait's parameters  $H'$  ranged about from 56 to 74.5 km and  $\beta$  ranged about from  $0.27$  to  $0.87 \text{ km}^{-1}$  (Gavrilov et al. 2020).
- 8) X1.5 of 14-12-2006 at 22:15UT; at low-latitude site in India: values of obtained Wait's parameters related to X1.5 depending on observed GCP are  $H'=59.6 \text{ km}$ ,  $\beta=0.512 \text{ km}^{-1}$  and  $H'=61.6 \text{ km}$ ,  $\beta=0.516 \text{ km}^{-1}$  compared to unperturbed conditions of  $H'=70.7 \text{ km}$ ,  $\beta=0.390 \text{ km}^{-1}$  and  $H'=71.0 \text{ km}$ ,  $\beta=0.390 \text{ km}^{-1}$  with estimated decrease in  $H'$  of 11.1 and 9.4 km and an increase in  $\beta$  of 0.122 and  $0.126 \text{ km}^{-1}$  (Kumar et al. 2015).
- 9) X1-X3.2 in period May–December 2013, all associated with CME and one of the weaker ones associated with SPE; at low-latitude site in Vietnam: values of obtained Wait's parameters for all cases of SFs are  $\beta$  increased from 0.3 to  $0.506 \text{ km}^{-1}$ , while  $H'$  decreased from 74 to 60 km (Tan et al. 2014).
- 10) X3-X5 in period 1994-1998, some associated with CME and SEP events; at mid latitude site at Dunedin, New Zealand: values of obtained Wait's parameters related to X3.0 estimated a decrease in  $H'$  of 12 km and an increase in  $\beta$  of  $0.13 \text{ km}^{-1}$  relative to their normal daytime values, from 71 to 59 km and from  $0.39$  to  $0.52 \text{ km}^{-1}$ , while for X5 is estimated decrease in  $H'$  of 13 km and the same increase in  $\beta$  (from 71 to 58 km and from  $0.39$  to  $0.52 \text{ km}^{-1}$  (McRae and Thomson 2004).

Results from this study, related to high-class SFs, fit well to the general linear trend across entire C–X-class range of X-ray SFs, obtained through numerical modeling based on VLF signal subionospheric propagation monitored on short path signals and recorded by Belgrade VLF station in wide time period, covering 14 years (from 2003 to 2017). These results are in line with results obtained by other research groups dealing with VLF data recorded in other mid-latitudinal sectors with similar position as Belgrade station. However, for some cases of X-class events, there is evident significant discrepancy in obtained results, probably due to latitudinal factor (like these reported by Pandey et al. 2015, Gavrilov et al. 2020 and Venkatesham and Singh 2018). Ionospheric response to analyzed high-class SF events from September 2017 was dramatic, in terms that estimated electron density in peaks of X-ray flux for both events exceeded its regular value for several orders of magnitude at the arbitrary height of 74 km, with about one order of magnitude difference within entire D-region altitude range between the weaker and the stronger SF event. Modeled ionospheric parameters of sharpness and effective

reflection height, as well as estimated electron densities for analyzed cases of X-class SF events are in correlation with X-ray flux soft component released during these SFs, as recorded by GOES satellites.

## Acknowledgments

This work was funded by Institute of Physics Belgrade, University of Belgrade, through grant by the Ministry of Science, Technological Development and Innovations of Republic of Serbia. Thanks are to D. Šulić for instrumental setup.

## References

- Barta, V., Natras, R., Srećković, V., Koronczay, D., Schmidt, M., Šulic, D., 2022, *Front. Environ. Sci.*, 10.
- Bekker, S. Z., Ryakhovsky, I. A., Korsunskaya, J. A., 2021, *J. Geophys. Res. Space Phys.*, 126.
- Bilitza, D., Altadill, D., Truhlik, V., Shubin, V., Galkin, I., Reinisch, B., Huang, X., 2017, *Space Weather*, 15, 418–429.
- Budden, K. G., 1988, *The propagation of radio waves*, Cambridge Univ. Press UK.
- Chowdhury, S., Kundu S., Basak, T., Ghosh S., Hayakawa, M., Chakraborty S., Chakrabarti, S. K., Sasmal, S., 2021, *ASR*, 67, 1599–1611.
- Ferguson, A. J., 1998, *Computer program for assessment of long-wavelength radio communications*, Version 2.0., Technical document 3030, Space and Naval Warfare Systems Center, San Diego CA 92152-5001, USA.
- Gavrilov, B. G., Ermak, V. M., Lyakhov, A. N., Poklad, Y. V., Rybakov, V. A., Ryakhovsky, I. A., 2020, *Geomagn. Aeron.*, 60, 747–753.
- Grubor, D. P., Šulić, D. M., Žigman, V., 2008, *Ann. Geophys.*, 26, 1731–1740.
- Grubor, D., Šulić, D., Žigman, V., 2007, *Proceedings of the IUGG XXIV General Assembly*, Perugia, Italy, July 2-13 2007.
- Hargreaves, J. K., 1992, *The solar-terrestrial environment*, Cambridge Univ. Press.
- Kolarski, A., Srećković, V. A., Mijić, Z. R., 2022, *Appl. Sci.*, 12, 582.
- Kolarski, A., Veselinović, N., Srećković, V. A., Mijić, Z., Savić, M., Dragić, A., 2023, *Remote Sens.*, 15, 1403.
- Kolarski, A., Grubor, D., 2021, *Proceedings of the The XIX SERBIAN ASTRONOMICAL CONFERENCE*, Belgrade, Serbia, October 13-17 2020, 387-390.
- Kumar, A., Kumar, S., 2018, *EPS*, 70-29.
- Kumar, S., Kumar, A., Menk, F., Maurya, A. K., Singh, R., Veenadhari, B., 2015, *J. Geophys. Res. Space Phys.*, 120, 788-799.
- McRae, W. M., Thomson, N. R., 2000, *JASTP*, 62, 609–618.
- McRae, W. M., Thomson, N. R., 2004, *JASTP*, 66, 77–87.
- Mitra, A. P., 1974, *Ionospheric effects of solar flares*. Astrophysics and Space Science Library, vol. 46, D. Reidel publishing Company, Boston, USA.

- Nina, A., Čadež, V. M., Bajčetić, J., Mitrović, S. T., Popović, L. C., 2018, *Sol. Phys.*, 293, 64.
- NOAA National Centers for Environmental Information. Available online: <https://satdat.ngdc.noaa.gov/sem/goes/data/avg/> (accessed on 15 August 2023).
- Pandey, U., Singh, B., Singh, O. P., Saraswat, V. K., 2015, *Astrophys. Space Sci.*, 357, 35.
- Silber, I., Price, C., 2017, *Surv. Geophys.*, 38(2), 407–441.
- Srećković, V. A., Šulić, D. M., Ignjatović, L., Vujčić, V., 2021, *Appl. Sci.* 11, 7194.
- Šulić, D., Srećković, V. A., 2014, *SAJ*, 188, 45-54.
- Tan, L. M., Thu, N. N., Ha, T. Q., Marbouti, M., 2014, *IJRSP*, 43, 197-246.
- Thomson, N. R., 1993, *JASTP*, 55 (2), 173–184.
- Thomson, N. R., Clilverd, M. A., Brundell, J. B., Rodger, C. J., 2021, *J. Geophys. Res. Space Phys.*, 126.
- Thomson, N. R., Rodger, C. J., Clilverd, M. A., 2005, *JGR*, 110, A06306.
- Thomson, N. R., Rodger, C. J., Clilverd, M. A., 2011, *JGR*, 116, 11305–11310.
- Venkatesham, K., Singh, R., 2018, *Curr. Sci.*, 114, 1923-1926.
- Wait, R. J., 1970, *Electromagnetic Waves in Stratified Media*, Pergamon Press, Oxford, UK.
- Wait, R. J., Spies, K. P., 1964, *Characteristics of the Earth-Ionosphere waveguide for VLF radio waves*, NBS Technical Note 300, USA.
- Whitten, R. C., Poppoff, I. G., 1965, *Physics of the Lower Ionosphere*, Englewood Cliffs, N.J. Prentice-Hall, USA.
- Žigman, V., Dominique, M., Grubor, D., Rodger, C.J., Clilverd, M.A., 2023, *JASTP*, 247, 106074.